JOURNAL OF GEOPHYSICAL RESEARCH, VOL. ???, NO. , PAGES 1–27,

Predicting Pacific decadal variability

Richard Seager, Alicia R. Karspeck, Mark A. Cane, Yochanan Kushnir

Lamont-Doherty Earth Observatory of Columbia University

Alessandra Giannini

International Research Institute for Climate Prediction

Alexey Kaplan, Ben Kerman and Jennifer Miller

Lamont-Doherty Earth Observatory of Columbia University

R. Seager, A. R. Karspeck, M. A. Cane, Y. Kushnir, A. Kaplan, B. Kerman and J. Miller, Lamont-Doherty Earth Observatory of Columbia University, Palisades, NY 10964-8000, USA. (address email to: rich@maatkare.ldeo.columbia.edu)

A. Giannini, International Research Institute for Climate Prediction, Palisades, NY 10964-8000, USA. (alesall@iri.columbia.edu)

Abstract

The case is advanced that decadal variability of climate in the Pacific sector is driven by tropical atmosphere-ocean interactions and communicated to the extratropics. It is shown that tropical decadal variations in the last century *could* arise as a consequence of the regional subset of physics contained within an intermediate model of the El Niño-Southern Oscillation. These decadal changes in ENSO and tropical mean climate are more predictable than chance years in advance but even in these idealized experiments forecast skill is probably too small to be useful.

Observations and atmosphere general circulation models are interpreted to suggest that decadal variations of the atmosphere circulation over the North Pacific between the 1960s and the 1980s are explained by a mix of tropical forcing and internal atmospheric variability. This places a limit on their predictability. The ocean response to extratropical atmosphere variability consists of a local response that is instantaneous and a delayed response of the subtropical and subpolar gyres that is predictable a few years in advance.

It is shown that the wintertime internal variability of the Aleutian Low can weakly impact the ENSO system but its impact on decadal predictability is barely discernible.

1. Introduction

For four years prior to fall 2002 the mid-latitudes of both the Northern and Southern Hemisphere experienced substantially less rain than usual. In the United States and across Southern Europe into Central Asia wells ran dry, crops failed and forests caught fire. The causes of this dry period have been linked to variations of the tropical atmosphere-ocean system in the Indo-Pacific region [*Hoerling and Kumar*, 2003]. After the enormous El Niño of winter 1997/98 the equatorial Pacific remained cooler than usual until early 2002 when a weak El Niño developed. It could be that this cold period marks the end of the most celebrated decadal variation in the Pacific sector: the warm shift in 1976 [*Zhang et al.*, 1997].

After 1976 the tropical Pacific Ocean has been warmer than in the preceding decades while the central and western North Pacific Ocean has been colder. In the atmosphere the post 1976 period has been characterized by low pressure over the mid-latitude North and South Pacific Oceans. In the early 1940s the climate of the Pacific went through a shift in the opposite direction. These characteristics of Pacific Decadal Variability (PDV) have been described by, among others, *Graham* [1994], *Trenberth and Hurrell* [1994], *Zhang et al.* [1997], *Mantua et al.* [1997] and *Garreaud and Battisti* [1999].

Decadal variations of the Pacific climate have important consequences for climate over land analogous, but not identical, to the impacts of the El Niño-Southern Oscillation (ENSO) on interannual timescales. For example *Mantua et al.* [1997] show that when the tropical Pacific is warm (e.g. after 1976) winters are warm across most of North America but cold in the

southeastern United States. Winters are dry across mid-latitude North America but are wet in the southwestern United States and Mexico. The persistent climate anomalies exert an impact on energy usage and power generation, agriculture and water resources. *Mantua et al.* [1997] also document an impressive correlation between PDV and North Pacific fish stocks. Decadal variations of ENSO have also been associated with decadal variations in Australian climate [*Power et al.*, 1999] and the strength of the Indian monsoon [*Krishnamurthy and Goswami*, 2000; *KrishnaKumar et al.*, 1999]. Because of the strong links between decadal ENSO variability and global climate variability predictions of the state of the Pacific climate on timescales of years to a decade or more could have significant human benefits.

Most work has been motivated by the idea that the adjustment time for the tropical Pacific Ocean is on the order of years and explains interannual variability and that, analogously, PDV must be associated with a different, decadal timescale, ocean process. This led naturally to explanations that PDV originated in the mid-latitude ocean-atmosphere system [*Latif and Barnett*, 1994, 1996]. It was then postulated that changes in the mid-latitude ocean were communicated through the ocean to the tropics, introducing a delay of several years and coupling together mid-latitude and tropical variability [*Gu and Philander*, 1997]. This has been shown, quite conclusively, not to work because the subsurface temperature signal becomes too weak [*Schneider et al.*, 1999]. In contrast, it has been shown that decadal variations of the tropical Pacific Ocean can be accounted for by tropical and subtropical wind forcing alone [*Schneider et al.*, 1999; *Karspeck and Cane*, 2002; *McPhaden and Zhang*, 2002]. This leaves the causes of the decadal changes of the tropical winds unexplained.

To go with the idea that PDV can originate in the tropics, there is ample evidence that extratropical climate variability in the Pacific can be explained in terms of tropical forcing. *Trenberth and Hurrell* [1994] made this case on the basis of observational analysis. Using atmosphere general circulation models (GCMs) forced by imposed SST variations in the tropical Pacific, but coupled to a mixed layer ocean elsewhere, *Alexander et al.* [2002] demonstrate that much of the North Pacific SST variability on both interannual and decadal timescales can be explained as a remote response to tropical forcing.

Here we will argue that PDV originates through coupled interactions of the tropical Pacific atmosphere-ocean system and is communicated through the atmosphere to the higher latitude Pacific. We also examine the predictability of PDV. Within the context of the proposed PDV paradigm we will ask:

1. Are decadal changes of the tropical Pacific atmosphere and ocean predictable?

2. Can the extratropical atmospheric response to decadal variations of tropical SST be simulated?

3. Can the response of the extratropical oceans to wind stress variations forced from the tropics be predicted some years in advance?

This leaves one interesting stone unturned. *Pierce et al.* [2000] and *Vimont et al.* [2001, 2003] have argued that variability of the North Pacific atmosphere circulation can cause trade wind variability that changes subtropical SSTs and impacts ENSO. Consequently we will also examine the impact on coupled tropical Pacific climate variability of that part of trade wind

variability that is associated with the internal, unforced, variability of the extratropical atmosphere.

2. Tropically generated Pacific decadal variability and its predictability

Until proven otherwise, a valid hypothesis for the origin of PDV is that it originates in the tangle of coupled atmosphere-ocean processes within the tropical Pacific that also give rise to interannual ENSO variability. This could arise in two ways. First, the longer timescale modes may arise deterministically (albeit chaotically) from nonlinear interactions among components of interannual variability. Second, the application of noise to a system that can only oscillate on interannual timescales will generate variability on decadal timescales. The second method is by definition not predictable on decadal timescales while the first may be if the slow evolution of the ocean state can be predicted.

2.1. Decadal variability in the Zebiak-Cane model

Here we consider the first possibility and examine decadal variations found within the Zebiak-Cane (ZC) model and their predictability (see *Karspeck et al.* [2003] for a more detailed account). The ZC model is a geophysical model of the tropical Pacific Ocean and the atmosphere above that is used for studies of ENSO and ENSO prediction [*Zebiak and Cane*, 1987; *Cane et al.*, 1986]. These references contain a complete model description.

Karspeck et al. [2003] demonstrated that the model is capable of creating realistic decadal variability by searching 150,000 years of simulated unforced natural variability for periods that matched observations. Figure 1 (top) shows one of dozens of 30 year model segments that

resemble the observed NINO3 record for the 1961 to 1991 period containing the 1976 warm shift, the unquestioned star of tropical decadal variability. This example has a correlation coefficient with the observed record of 0.59 (using unfiltered monthly data) and has a post 1976 warming (relative to the 15 years before) of $0.41°C$ compared to the observed $0.38°C$. The other two examples shown have equally high correlation to observations and are the 1942 'cold shift' ($-0.36°C$ shift in the model compared to the observed $-0.32°C$) and, for comparison, a 'neutral shift' centered on 1903 (neither model nor observations had a noticeable shift). Each of these decadal variations can be mimicked by the model. The lesson is that the regional subset of tropical climate physics contained within the ZC model may be sufficient to generate the decadal variations that have occurred in the last 150 years.

2.2. Predictability of decadal variability in the Zebiak-Cane model

To assess the predictability of the decadal variations in the model we identified twenty four 30 year segments (hereafter called model analogs) for each of the three observed segments (i.e. those centered on 1976, 1942 and 1903). The twenty four chosen were those with the highest correlation coefficient with the observed record (all ≥ 0.5) and with an appropriate size shift in the average temperature between the last and first 15 years of the record ($0.3°C$ for warm shift, $-0.3°C$ for the cold shift and absolute value $\leq 0.1°C$ for the neutral shift).

To assess the predictability of these events an ensemble of 100 forecasts was run for each of the model analogs. Each forecast was initialized 5 years prior to the shift (e.g. in January 1971 for the analogs of the 1976 shift) and integrated for the subsequent 20 years. The initial

condition was the exact state of the model analog at the beginning of the forecast plus a random perturbation in the SST anomaly field. The SST perturbation is uncorrelated in space. The magnitude is randomly taken from the statistical distribution of the SST anomaly at that grid point evaluated from the 150,000 year integration. Given these perturbations any predictability of the decadal shifts must be gained from large scale and coherent ocean structures that are not disrupted by the application of noise.

The criteria for evaluating whether the forecasts are right or wrong are shown in Figure 2. A forecast of the warm shift analogs would be 'correct' if the later 15 years were warmer than the earlier 15 years by more than $0.21°C$, 'weakly correct' if they were between $0.06°C$ and $0.2°C$ warmer and plain 'wrong' if the later years were less than $0.06°C$ warmer, or actually colder, than the prior 15 years. These numbers were taken by dividing the statistical distribution of shifts in the 150,000 year run into quintiles with equal numbers of shifts in each. The 'wrong' category covers three quintiles. The success of forecasts of the cold and neutral shifts are defined analogously and also illustrated in Figure 2.

Table 1 shows the frequencies of correct, weakly correct and wrong forecasts for the warm, cold and neutral shifts, expressed in percentages. The model has definite skill at predicting warm shifts: less than 20% of the forecasts are wrong while almost 60% are correct. The model seems to have less skill at predicting cold or neutral shifts but still two thirds of the forecasts shift in at least the right sense.

2.3. Comparing decadal predictability in the Zebiak-Cane model with that from statistical forecasting strategies

Does the skill of the decadal predictions with the ZC model beat what could be obtained from simple statistical forecasts? We know that the irregularity in the ZC model arises not from noise but from its internal, deterministic dynamics (e.g. *Tziperman et al.* [1995]). Does this dynamics provide any predictability beyond what is expected by chance?

Two statistical prediction schemes were used as strawman-null hypotheses. One uses the statistical distribution of model states and randomly grabs the twenty years after a forecast start from this distribution. Forecast skill in this scheme rests on a statistical tendency to shift away from extreme states toward the model mean. The second scheme uses a noise-forced, seasonal, second order autoregressive [AR(2)] model (which allows an oscillation) fitted to the ZC model. As for the ZC model, analog segments of observed decadal variability were located in a 150,000 year run of the AR(2) model and then ensemble forecasts were performed using different sequences of noise forcing for the 20 years after the forecast initialization. Comparing to this model asks whether the ZC model predictability improves on that of the simplest characterization of ENSO.

As shown in Table 1 the two statistical forecasting schemes have some skill at predicting warm shifts but the ZC model outperforms them for all shifts by a modest amount. To assess by how much the ZC model skill exceeds what would be expected by chance we used the Ranked Probability Score (RPS, [*Wilks*, 1995]). In contrast to merely counting up the number of successful forecasts, the RPS accounts for how far the forecast is from what actually happened.

For each forecast system we compute the fraction correct (f_c), the fraction weakly correct (f_{wc}) and the fraction wrong (f_w) with $f_c + f_{wc} + f_w = 1$. Then the RPS is given by:

$$RPS = (f_c - 1)^2 + (f_c + f_{wc} - 1)^2. \quad (1)$$

If the forecasts are all correct then $f_c = f_c + f_{wc} = 1$ and $RPS = 0$. If they are all wrong then $f_c = f_c + f_{wc} = 0$ and $RPS = 2$. In between the RPS will get less (i.e. the forecast is better) even when f_c remains the same if f_{wc} increases, thus measuring that the forecasts became closer to the observed state.

We checked the ZC model skill scores against the distribution of scores obtained from 5000 100 member ensemble forecasts with each statistical scheme. The statistical distributions of the 5000 RPSs for the statistical schemes for the warm shift, cold shift and neutral shift are shown in Figure 3. The RPSs for the ZC model are shown as vertical bars. The RPSs for the ZC model are lower, i.e. the forecasts are more skillful, than could be accounted for by chance. The ZC model clearly beats the statistical forecast techniques albeit by a modest amount.

2.4. Discussion

For warm, neutral and cold shifts the ZC model predictions have greater skill than statistical predictions. The greatest skill is for warm shifts. However the statistical models also have skill at predicting warm shifts. This arises from knowing at forecast initialization time that conditions have been colder than normal and that the subsequent 20 years are, statistically speaking, likely to be more akin to climatology [*Karspeck et al.*, 2003].

With only 150 years of observed ENSO variations it is impossible to know the true statistical distribution of decadal shifts. Our statistical model was based on the 150,000 years of model ENSO variability. A statistical model based on only the observational record would probably be a poor tool for decadal prediction, notably worse than the ZC model.

Since the decadal predictability of the ZC model exceeds that of the statistical forecasting techniques we conclude that at least some of the decadal predictability within the model arises from its decadally varying (ocean) state. In that the model can mimic the observed decadal changes this raises the possibility that tropical Pacific decadal variability can arise from aspects of the ocean adjustment that are modestly predictable several years in advance.

To wrap matters up we performed a 1000 member ensemble of 30-year real world forecasts using the ZC model. The forecasts were initialized in December 2002 using the operational data assimilation method outlined in *Chen et al.* [2000]. The initial state of each ensemble member differed by the addition of a random (uncorrelated in space) perturbation of the SST and the sea level height fields with standard deviation of $3^{\circ}C$ and 3cm respectively. Of most interest was the difference in NINO3 for the 15 year period after 1998 minus the 15 year period before. In this statistic the observed NINO3 was used from 1983 to 2002 and forecast NINO3 for 2003 to 2013. Using the same divison of shifts into quintiles as before, none of the 1000 forecasts went warm or weakly warm, 2.2% showed no shift, 56.8% went weakly cold and 41% went cold. The model, at least, is convinced that the 1997/8 El Niño marked the end of the post-1976 warm period.

3. Predicting decadal variations of extratropical atmosphere circulation from known SSTs

The previous section raises some hope that decadal variations of tropical Pacific climate may be predictable to a modest degree years in advance. Will this advance knowledge allow the prediction of decadal climate variations outside of the tropical Pacific? On the interannual timescales it is well known that the movement of regions of deep convection that occurs within the ENSO cycle forces changes in the tropospheric stationary and transient eddies that create climate anomalies worldwide [*Horel and Wallace*, 1981; *Ropelewski and Halpert*, 1987, 1989; *Sardeshmukh and Hoskins*, 1988; *Held et al.*, 1989; *Hoerling and Ting*, 1994]. It is not so well established that decadal variations of tropical SSTs have an analogous impact.

Decadal variations of atmosphere circulation in the Pacific sector can be easily seen by looking at the difference between averages of the decade after the 1976 warm shift and the decade before. In Figure 4a we show the differences in SST during November to March for the period 1977/1978 to 1986/1987 minus the period 1966/1967 to 1975/1976. In Figure 4b we show the difference in 500mb geopotential height for the same season and periods.

After 1977 the Aleutian Low was anomalously deep. This was a typical equivalent barotropic signal as evidenced by anomalously low sea level pressure (SLP) below and shifted to the east (not shown). There was anomalous high geopotential height over North America centered in the northwest. Associated with this circulation shift there was cold water stretching from the coast of Japan to the central North Pacific while the tropics were warm, especially in the east. The SST pattern is very similar to the decadal 'ENSO-like' pattern of *Zhang et al.* [1997] with

the warmest SST anomalies being just south of the Equator and the tropical and mid-latitude anomalies being of equal magnitude. In the SST field there is a suggestion of hemispheric symmetry (see *Seager et al.* [2003]) although this should not be too marked given that we are looking at northern winter and southern summer together.

The pattern of decadal variability of atmosphere circulation identified in Figure 4 could arise due to internal variability of the atmosphere or could be boundary forced by variations in SST. A useful first step is to compare the decadal variations with the interannual ones. Figure 5 shows the 500mb height anomaly for the November through March season regressed onto the NINO3 index, using data from the NCEP-NCAR Reanalysis for 1959 to 1999. Given the number of El Niño and La Niña events in this time period it is reasonable to assume that the pattern shown in Figure 5 is that of the ENSO-forced 500mb variability.

It is quite similar to the pattern of decadal variability. Both have low geopotential over the North Pacific (although the decadal low is 20° west of the interannual low) and both have high geopotential over North America and in the tropics. The proportionality between the tropical and mid-latitude height anomalies is similar for both patterns which is strong circumstantial evidence for tropical forcing of each.

To further examine whether the observed decadal variations of the extratropical atmosphere are caused by internal variability or are boundary forced we performed an ensemble of 48 simulations with the National Center for Atmospheric Research Community Climate Model version 3 (NCAR CCM3, [*Kiehl et al.*, 1998]). Each ensemble member had different initial

conditions but each used the same history of observed SSTs as a lower boundary condition from 1959 to 2000. The SST data used is that of the Hadley Centre [*Rayner et al.*, 2003].

For a sufficiently large ensemble, taking the ensemble mean removes the internal variability leaving behind the boundary-forced component. To check this we divided the 48 member ensemble into three groups of 16. The temporal and spatial patterns of variability in the ensemble mean of each group were nearly identical. Results are shown here for one 16 member group.

Figure 6 shows the ensemble mean 500mb height anomaly for the November through March season regressed onto the model NINO3 index for 1959 to 1999. The model pattern is very similar to that observed (Fig. 5) both in terms of the spatial location of principal features and in their amplitude. This confirms that the observed pattern is boundary-forced and that the model has some skill at reproducing this signal.

Figure 7 shows the model ensemble mean 500mb height difference for the decade after 1977/78 minus the decade before. The model decadal difference over the tropical and North Pacific is only about one half of that observed (Fig. 4b) while the spatial patterns are very similar. Two explanations for why the modeled shift is weak come to mind.

First, the model-data comparison could be taken to indicate that the observed decadal difference is the sum of a small SST-forced component and a much larger component due to internal atmosphere variability. For example in Figure 8 we show the same decadal difference of 500mb geopotential height in an individual member of the ensemble that captures the pattern and magnitude of the extratropical decadal shift. However, the amplitude of the associated tropical

shift remains weak (as in every other ensemble member). This suggests that the decadal shift in this ensemble member is the sum of large internal variability and a small SST-forced shift.

Second, the weak tropical $500mb$ height shift may cause the weak extratropical response. Shifts in $500mb$ height can be caused by shifts in surface pressure and/or tropospheric temperature between the surface and $500mb$. As shown in Figure 9a, the model fails to capture the increase in lower tropospheric thickness temperature (evaluated between the surface and $500mb$) that occured in 1977 and persisted through 1984. This is the main cause of why the decadal shift in modeled tropical $500mb$ height shown in Figure 7 is smaller than that observed (Figure 4b). What is more, the model also fails to simulate the high surface pressure in the seven years following 1976 (Figure 9b). The observed increase in surface pressure at this time is found in the Reanalysis, the recent Hadley Centre SLP analysis [*Basnett and Parker*, 1997] and the analysis (following the procedure of *Kaplan et al.* [2000]) of the most recent release, in 2001, of the COADS surface pressure data from ships and buoys [*Woodruff et al.*, 1998] (also shown in Fig. 9b). On the other hand the Reanalysis has a long term increase in the tropical mean surface pressure that is not in CCM3 or the two other surface pressure data sets and is probably spurious. This would effect comparisons between models and the Reanalysis of decadal changes from the 1960s to the 1980s.

A 24 member ensemble with the ECHAM4.5 atmosphere GCM conducted by the International Research Institute for Climate Prediction, and with SST-forcing everywhere, has a decadal shift across 1976 that is very similar to that of CCM3. It underestimates the decadal shift everywhere,

misses the increase in tropical thickness temperature and surface pressure after 1976 and has no long term increase in surface pressure.

3.1. Discussion

Given these considerations the fixed proportionality in the Reanalysis between tropical and North Pacific height changes going from interannual to decadal variability (compare Figures 4b and 5) remains suggestive of tropical forcing of both. However, the reversal to a weaker Aleutian Low in the late 1980s did not correspond to any persistent tropical change and is most likely due to internal variability. Returning to prediction, the inability of the two atmosphere GCMs to capture the jump in tropospheric temperatures and sea level pressure in 1977 makes it clear that even state of the art GCMs have a hard time simulating the tropical atmosphere response to decadal variations of tropical SST. The consequences of this error for the extratropical atmosphere circulation are not immediately apparent.

There is another possibility for why the decadal shift in the height anomalies over the North Pacific is smaller than observed. The post 1976 period is also characterized by warmer Indian Ocean SSTs. In nature these are usually caused, in part, by increased downward solar radiation [*Klein et al.*, 1999] associated with *reduced* precipitation. Consistently, *Deser et al.* [2003] have shown that the post 1976 period had less cloud cover, and therefore presumably less precipitation, in the North Indian Ocean where the SST was warmer. *Barsugli and Sardeshmukh* [2002] have shown that reduced atmospheric heating in this region should cause lowered 500mb heights over the North Pacific, amplifying the impact of the increased heating over the central tropical

Pacific Ocean. In the model however, specifying the warm SST anomalies in the Indian Ocean caused increased precipitation (not shown) forcing a wave train that would partially cancel that forced by tropical Pacific Ocean heating anomalies.

This idea gains some support from a comparison of two 5 member ensembles conducted with CCM3 at the National Center for Atmospheric Research (not shown). One ensemble was forced with observed SSTs everywhere and is analogous to our ensemble and also had increased precipitation over the Indian Ocean after 1976. The other was forced with observed SSTs in the tropical Pacific Ocean and computed the SST anomalies with a mixed layer ocean elsewhere. This one had no increase in precipitation over the Indian Ocean after 1976 and, consistent with the reasoning above, the 500mb height drop over the North Pacific was larger than in the ensemble with SST-forcing everywhere. However, a larger ensemble is needed to prove the point that imposing Indian Ocean SST anomalies can lead to a mis-estimate of the extratropical response to tropical forcing.

4. Predicting the response of the North Pacific Ocean to decadally varying winds

Tropically-forced wind anomalies over the North Pacific will generate an ocean response. The simplest part of this is generated by anomalous surface fluxes. For example, if the tropics force a deeper Aleutian Low, stronger wind speeds on the southern side of the Low would tend to increase the latent heat flux and tend to cool the SST. To the east, along the North American coast, southerly wind anomalies would tend to warm the SST by warm, moist advection. In the western North Pacific cold, dry advection would tend to cause cooling [*Cayan*, 1992a, b].

Only slightly more complex, there is a response in the Ekman component of the ocean currents. Continuing with the example of a tropically-forced deep Aleutian Low, stronger westerlies at about $35°N$ cause anomalous southward currents. These are located in a region of strong meridional mean SST gradients and cool the SST. *Seager et al.* [2001] used an ocean GCM to show that this is actually the *dominant* term causing central Pacific SST anomalies on interannual and decadal timescales, overwhelming the surface flux forcing (see also *Miller et al.* [1994]).

If the anomalous winds over the North Pacific can be predicted so can these local components of the SST response, both of which develop within a day or two.

More complex is the response of the ocean gyre circulations to persistent decadal changes in the North Pacific atmosphere circulation. In the decade after 1976 the Aleutian Low was stronger and to the south of its location in the preceding decade [*Seager et al.*, 2001] which caused the latitude separating the subtropical and subpolar gyres to also shift south. Just east of Japan the dividing latitude between these gyres is marked by the Kuroshio-Oyashio Extension (KOE), separating warm subtropical waters to the south from cool subpolar waters to the north. When the KOE shifted south in the 1980s a potent cold SST anomaly developed in the region it had evacuated as the latitudinal distribution of ocean heat transport altered.

Seager et al. [2001] showed that KOE SST anomalies developed a few years after those in the central Pacific, consistent with the time for westward propagation of oceanic Rossby waves from the region of wind stress forcing. Thus the two modes of SST variability in the North Pacific are not independent (in contrast to *Nakamura et al.* [1997]); both are responding to

the same variations in winds but the central Pacific response is instantaneous and local while the KOE response is delayed and remote.

The delayed response of the gyre circulation has been exploited by *Schneider and Miller* [2001] to attempt hindcasts of SST anomalies east of Japan. They used a simple time dependent model of thermocline depth in which anomalies at any longitude and time are related to the anomalous wind stress forcing to the east by integrating back in time along Rossby wave characteristics. SST anomalies were then linearly related to thermocline depth anomalies. Hindcasts were performed by integrating the model forward with observed wind stress forcing to the time of the beginning of the hindcast and then continuing with zero wind stress anomaly. As the now unforced Rossby waves continued to propagate west they created thermocline and SST anomalies. *Schneider and Miller* [2001] validated the hindcast SST anomalies against observations (see Figure 11) to show that the hindcasts have modest skill out to a few years ahead.

While SST anomalies in the KOE region only have a limited subsequent impact on the atmosphere circulation, meaning that a mid-latitude coupled mode of oscillation in which the delayed response of the ocean provides for predictability is unlikely to rise above the noise, prediction of the ocean climate alone is important. *Miller and Schneider* [2001] have described the impacts that movements of the Kuroshio and Oyashio currents have on local marine ecosystems and fisheries.

5. The impact of internal variability of the North Pacific atmosphere on ENSO and its predictability

Vimont et al. [2001, 2003] have proposed that internal variability of the atmosphere over the North Pacific, essentially the strength of the Aleutian Low, is associated with variations of the northeast trade wind strength during winter and forces subtropical SST anomalies. They argue that the SST anomalies persist into spring and summer and are damped by anomalous surface fluxes forcing an atmosphere response that includes zonal wind anomalies on the Equator that excite the coupled ocean-atmosphere dynamics familiar in ENSO. Now we turn to an examination of the realism and significance of this mechanism of extratropical-tropical coupling.

It is difficult and perhaps impossible to use the observational record to separate between the pattern of atmospheric internal variability over the North Pacific and the pattern of tropically-forced variability. However this is easy to do using SST-forced atmosphere model ensembles. Using the same 16 member ensemble as before, removing the ensemble mean - the boundary-forced component - leaves behind 16 40-year long records of variability generated by internal atmosphere processes alone. We concatenated these records and performed a singular value decomposition analysis on the fields of surface wind speed and stress over the subtropical and tropical North Pacific ($0° - 30°N$) for the December through February mid winter period. The patterns are shown in Figure 12 and represent a strengthening and weakening of the northeast trades associated with variations of the Aleutian Low.

Stronger (weaker) trade winds will cool (warm) the subtropical SSTs via an increase (decrease) in the latent heat flux (Q_{LH}). In the absence of a change in ocean heat transport

(which to first order is reasonable for the subtropics) the wind-forced flux variations will be balanced by a compensating change in the latent heat flux due to the SST change. In equilibrium the latent heat flux change will be zero and,

$$\rho_a c_E L \bar{U} \Delta q' = -\rho_a c_E L \overline{\Delta q} U'. \tag{2}$$

Here $\bar{U}$ and $\overline{\Delta q}$ are the mean wind speed and air-sea humidity difference and U' and $\Delta q'$ are the changes in the same.

If the relative humidity remains fixed at a value close to δ [*Seager et al.*, 1988], then $\Delta q' \sim (1-\delta) q_s'$, where q_s' is the change in surface saturation specific humidity. q_s' can be linearized using the Clausius-Clapeyron relation as $q_s' \sim \left(\frac{\partial q_s}{\partial T_s}\right) T_s'$ where T_s' is the SST anomaly. The equilibrium SST anomaly induced by the wind anomaly U' is then given by:

$$\bar{U}(1-\delta)\left(\frac{\partial q_s}{\partial T_s}\right) T_s' = -\overline{\Delta q} U'. \tag{3}$$

If U' is varying in mid-winter, T_s' will develop into spring and then decrease as U' goes to zero and the SST-induced part of the latent heat flux damps the SST anomaly. There will be an atmospheric response to this damping. The Zebiak-Cane model is well-suited for testing the importance of this process. Both the atmosphere and ocean components of the model contain a surface flux anomaly that is proportional to T_s' as on the left hand side of Eq. 3 (but with a constant coefficient, α (see Eq. 4 below)). First we computed a latent heat flux anomaly from Eq. 4 using U' derived from the SVD analysis (Figure 12) and a climatological mean winter

values of $\overline{\Delta q}$. We then imposed this flux anomaly as aan initial condition in the Zebiak-Cane model and examined the response and the subsequent evolution of the coupled model over the next several months.

As shown in Figure 13, the latent heat flux anomaly induced a subtropical warming and a wind response consisting of southwesterly anomalies to the south. As explained by *Gill* [1980], heating north of the Equator forces descent and the vorticity balance requires that the vortex stretching be balanced by poleward advection of planetary vorticity, i.e. southerly flow. The westerly component arises from conservation of angular momentum in the northward flow. *Zebiak* [1982] shows that, when the heating north of the Equator is localized in longitude, the southwesterly anomaly extends onto the Equator. The initial ocean response has higher sea level height (SLH), or deeper thermocline, in the central Pacific. As the ocean response evolves (Figure 14), the equatorial southwesterlies force a downwelling oceanic Kelvin wave that propagates east raising SLH and depressing the thermocline in the eastern equatorial Pacific. This immediately causes SST warming in the east and a few months later a classic El Niño pattern develops (Figure 15), albeit with small amplitude, $\sim 0.3^{\circ}C$.

This simple experiment demonstrates that internal extratropical atmosphere variability can indeed excite coupled equatorial dynamics. It remains to be shown whether this impact is potent enough to influence ENSO evolution and decadal predictability. To do this we add a latent heat flux forcing term proportional to U' (c.f. the right hand side of Eq. 2) to the SST equation of the Zebiak-Cane model:

$$\frac{\partial T_s'}{\partial t} + dynamics = -\alpha T_s' + bU' f(t). \quad (4)$$

The term 'dynamics' is standing in for the three dimensional advection processes within the model mixed layer and the term $-\alpha T_s'$ is the model version of the processes damping SST anomalies (see *Zebiak and Cane* [1987]). The coefficient b is, for simplicity, taken to be a constant. The function $f(t)$ accounts for the time dependence of the wind speed forcing. It is zero between April and October and then increases to a maximum absolute value in January before declining. It has the same sign throughout each winter season to represent low frequency variability of the Aleutian Low but its value varies randomly from year to year according to a white noise process. Included in this way the subtropical wind speed anomaly will tend to generate an SST anomaly with maximum value in March that will be damped in the seasons following.

We proceeded as before. a long run of the model with the subtropical wind forcing imposed was generated and searched for analogs of the observed decadal variability. Hindcasts of these were conducted as before except that, rather than imposing SST perturbations at the start of the forecast, each forecast was continued with a different sequence of subtropical wind speed forcing. Forecast skill was assessed as before and the percent of 'correct', 'weakly correct' and 'wrong' forecasts for the warm, cold and neutral shifts are shown in Table 2. Table 2 also shows the performance of the two statistical forecasting strategies, both of which were regenerated using the data from the long, subtropical forced, model run.

Compared to the forecasts without noise-foring (Table 1) the percentage in each forecast category varies only slightly. The ZC model retains the same modestly higher level of skill compared to the statistical schemes. These experiments demonstrate that the skill of the ZC model, such as it is, is retained when realistic noise is continually applied during the forecast. That is, the continual noise is a no more disruptive process than the initial condition perturbations considered in Section 2.

6. Conclusions

We have investigated the causes of decadal variability of Pacific climate and its potential predictability. The conclusions are as follows:

• Decadal variations resembling observations in the tropical Pacific over the last 150 years or so can be generated by the regional subset of climate physics contained within a familiar intermediate model of the tropical Pacific alone. This does not prove that this physics is the cause of tropical Pacific decadal variability in the real world but it does make a case that it is not immediately necessary to invoke processes in other regions of the world.

• The model analogs of observed decadal variations, such as the 1976 warm shift, are predictable years in advance. The skill of the geophysical model significantly exceeds that of statistical schemes but is too modest to hold out much hope for useful decadal forecasts.

• Decadal variations of tropical Pacific climate drive decadal variations of extratropical climate that could be predicted if the changes in tropical SST were known. However, the observed decadal variations of extratropical climate over the North Pacific in the late twentieth century

also include a large component that is generated by unpredictable internal atmospheric processes. Furthermore, atmosphere models forced by observed SSTs everywhere poorly simulate the tropical response to decadal variations of SST.

• There is a component of the response of the extratropical North Pacific ocean to decadal variations of the winds that is instantaneous and local and can be predicted if the winds are known. There is another component that relates to the delayed adjustment of the subtropical and subpolar gyres. This component causes SST anomalies in the Kuroshio-Oyashio Extension region and is predictable on the timescale it takes for Rossby waves to propagate west to the Asian coast, that is, years.

• Internal wintertime variability of the atmosphere over the North Pacific is capable of changing wintertime trade wind strength and generating SST anomalies in the subtropics. During the subsequent spring and summer the tropical winds respond to the surface flux damping of this SST anomaly in a way that includes equatorial wind anomalies. These generate a coupled dynamical response that is ENSO-like but weak.

• The decadal predictability of the ZC model is not significantly perturbed by the application of subtropical forcing.

In summary, a case can be made that Pacific Decadal Variability arises through coupled interactions in the tropics and is communicated to the extratropics. Aspects of this variability are predictable years in advance but the skill is so low that the prospects for operational prediction are poor.

Acknowledgments. This work was supported by the National Oceanic and Atmospheric Administration (grants NA16GP2024 and UCSIO CU 02165401SCF) and by the National Science Foundation (grant ATM-9986072). We thank David Battisti and Clara Deser for valuable discussions, Dake Chen for guidance in hindcasting and forecasting and Ed Sarachik for first suggesting this work.

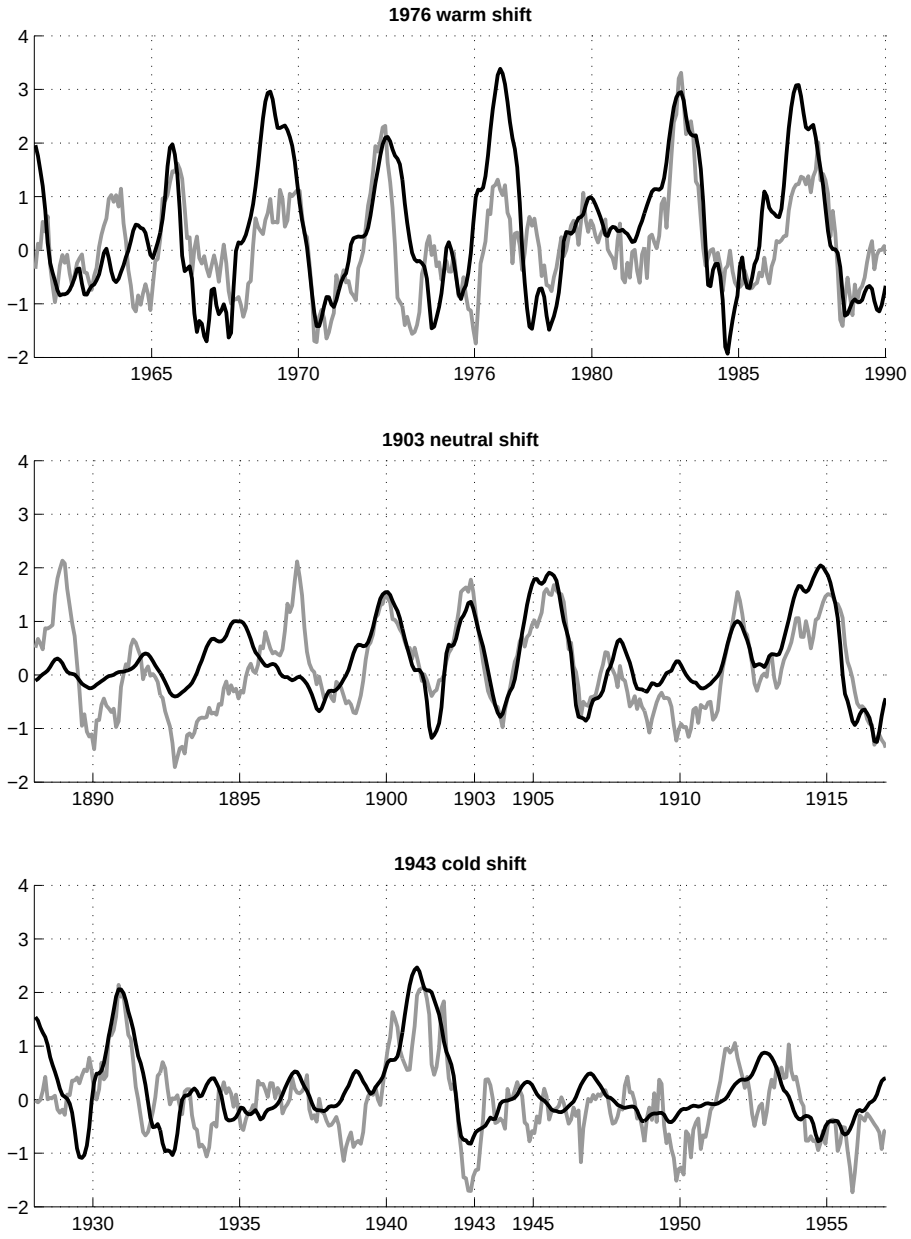

Figure 1. Time series of NINO3 from observations the Zebiak-Cane model. The model segments were chosen from the long run to match the observed interannual variability and the decadal shifts. The first has a warm shift across 1976 with the 15 years after being warmer than the 15 years before by $0.38°C$ (observed) and $0.41°C$ (model), the third has a cold shift across 1943 of $-0.32°C$ (model) and $-0.36°C$ and, for comparison, the second has no shift at all.

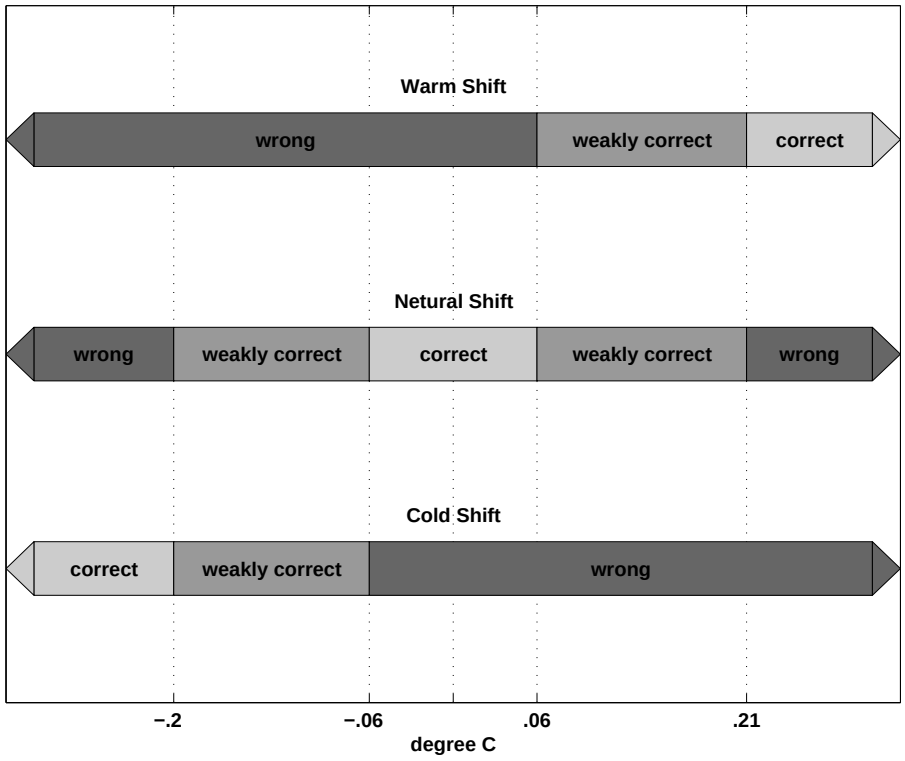

Figure 2. Schematic showing how forecasts are divided into 'correct', 'weakly correct' and 'wrong'.

Table 1. Performance of the dynamical model and two naive forecasting strategies presented as a function of the sense of the shift (warm, neutral or cold). Results for the dynamical model are based on 100 member ensembles for each of the 72 analog series (24 each of warm, neutral and cold shifts). Ensembles of size 500,000 were used for the naive forecasts.

	ZC Dynamical Forecasts			**Naive Reference Forecasts**					
				ZC-Long distribution			**AR(2)**		
	correct	*weak*	*wrong*	*correct*	*weak*	*wrong*	*correct*	*weak*	*wrong*
warm shift	59%	23%	18%	42%	26%	32%	47%	16%	37%
neutral shift	21%	45%	34%	18%	39%	43%	14%	30%	56%
cold shift	41%	23%	36%	30%	22%	48%	34%	14%	52%

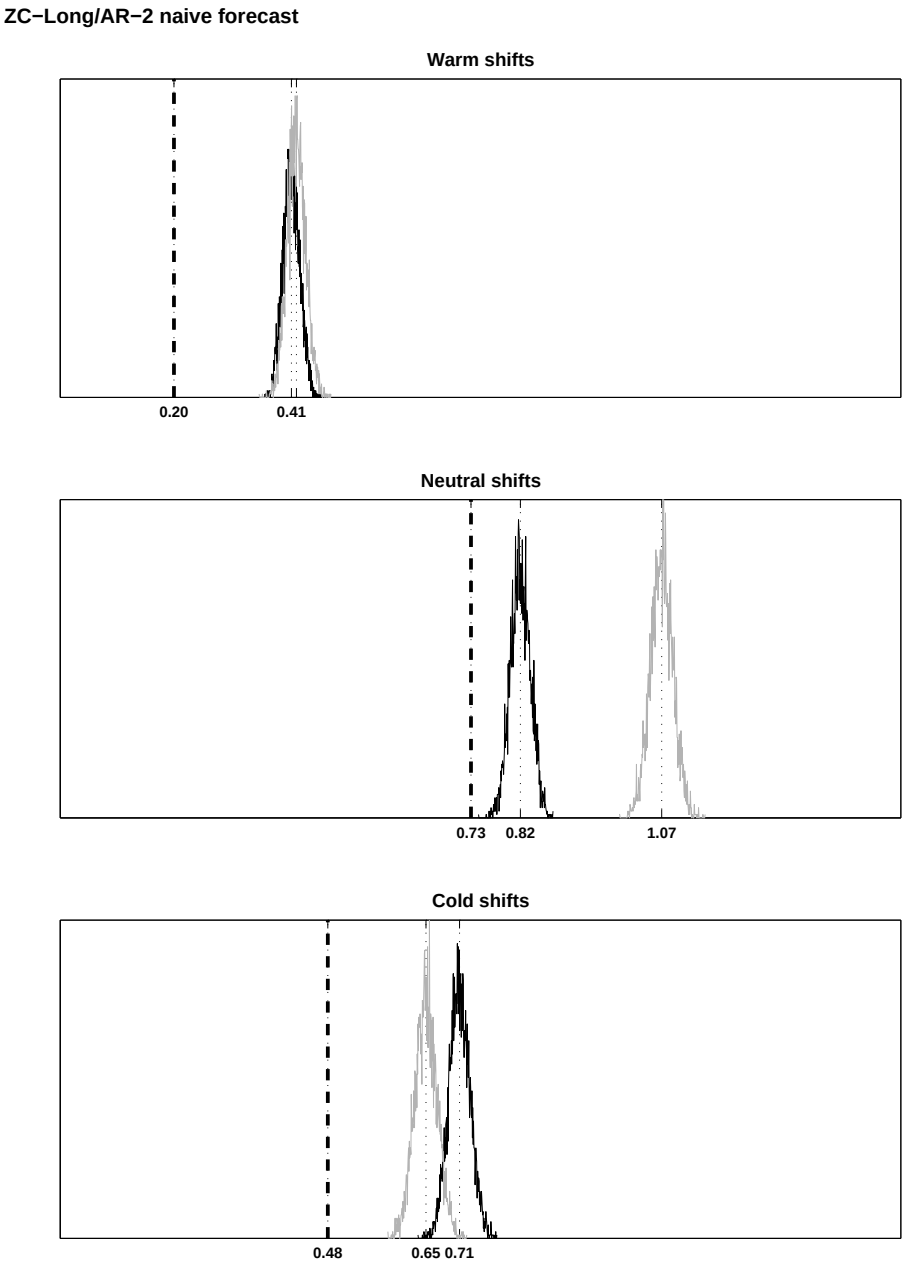

Figure 3. Ranked probability score for the warm shift, neutral shift and cold shift forecasts by the ZC model, the AR model (gray) and the naive strategy (black). The RPS scores for the two statistical methods are shown as a distribution of 5000 scores. The ZC scores are shown as a single vertical line. In each case the ZC forecasts are unambiguously more skillful (i.e. RPS closer to 0) than the statistical forecasts.

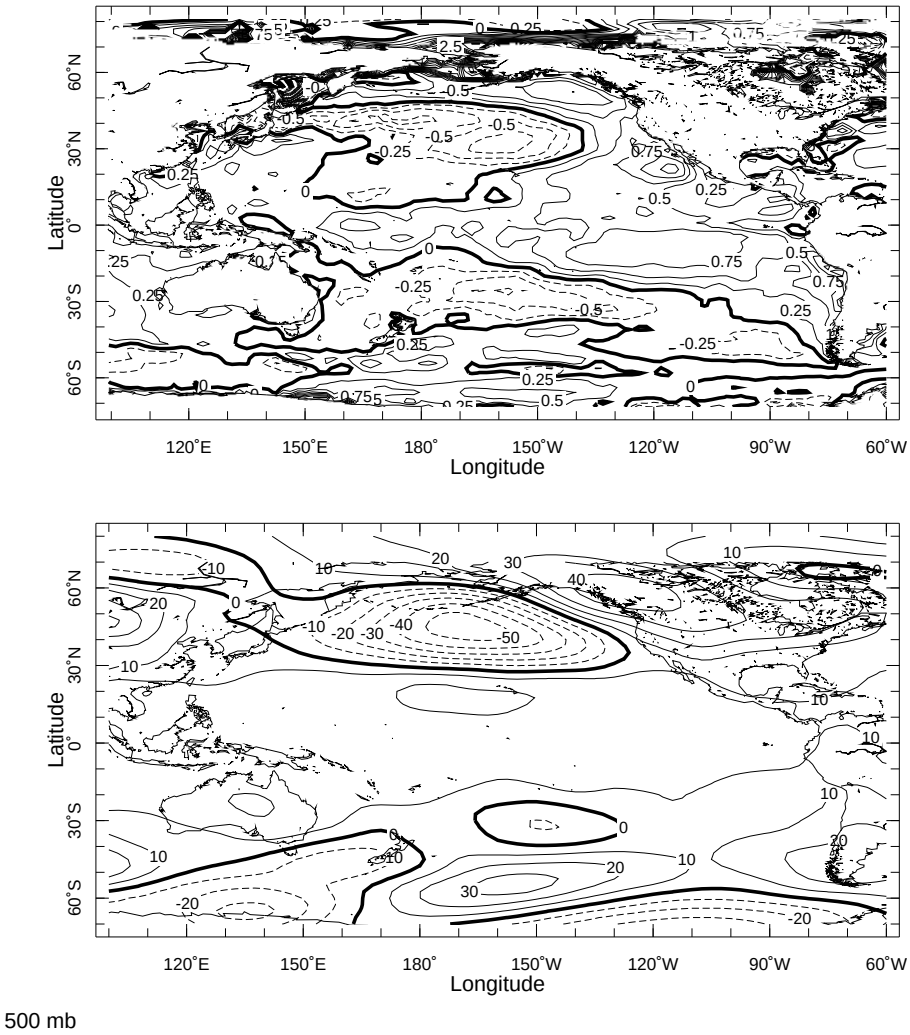

Figure 4. The difference in (a) SST and (b) 500mb height for the November to March season for the average of winters from 1977/78 to 1986/87 minus the average of winters from 1966/67 to 1975/76. The contours are in Kelvin for (a) and meters for (b). The data are from the NCEP Reanalysis. The increased heights in the tropics are probably overestimated (see text).

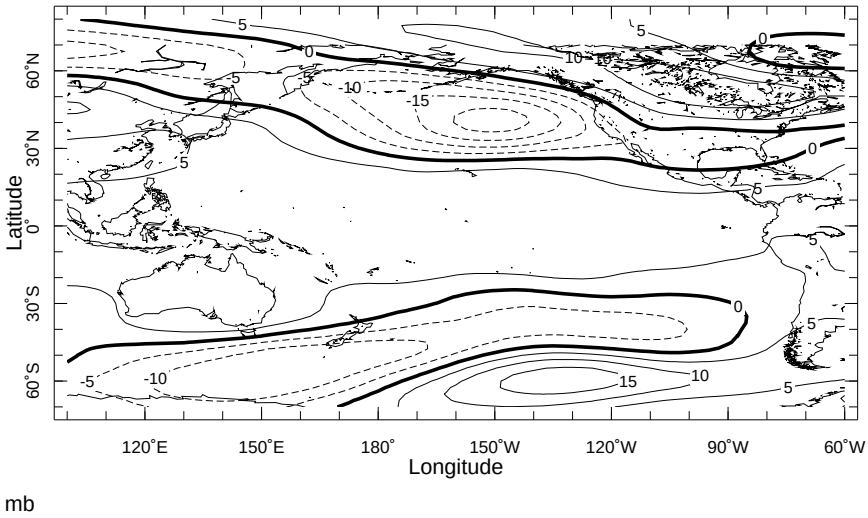

Figure 5. The 500mb height for the November to March season regressed onto the NINO3 index. Contours are meters and the data is from the NCEP Reanalysis.

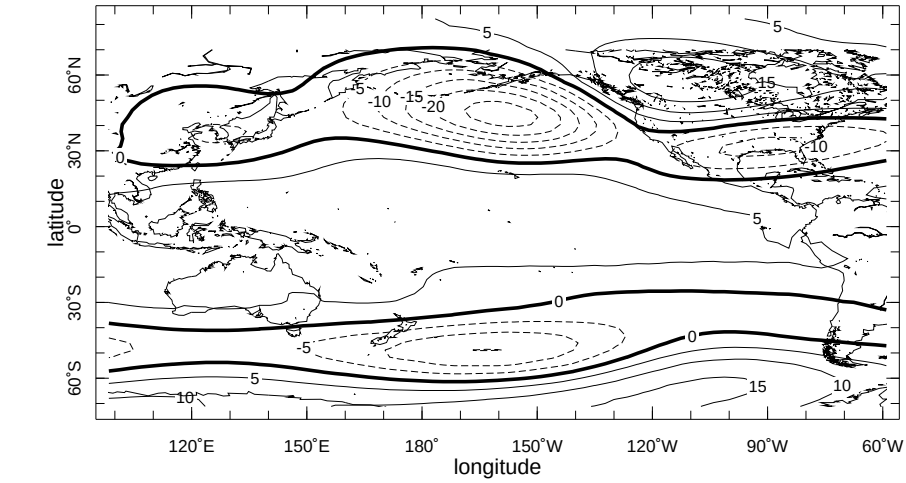

Figure 6. Same as Figure 5 but for the ensemble mean of 16 integrations of the CCM3 atmosphere model using observed SST in the surface boundary conditions.

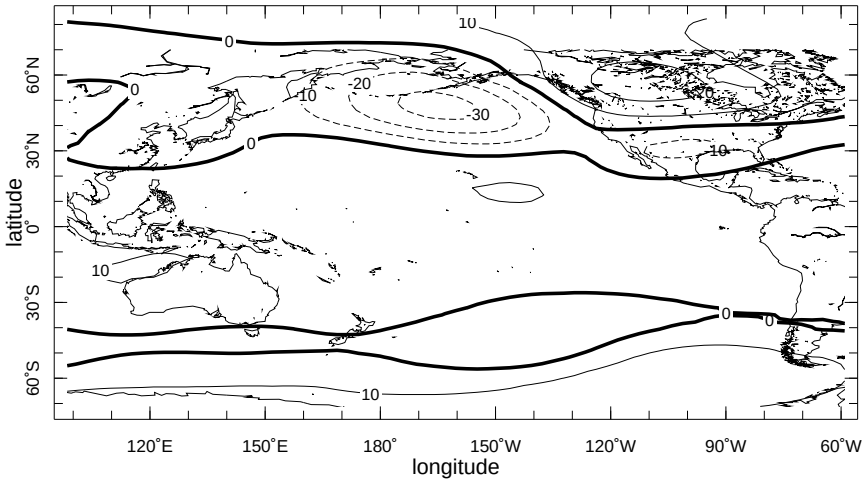

Figure 7. Same as Figure 4b but for the ensemble mean of 16 integrations of the CCM3 atmosphere model using observed SST in the surface boundary conditions.

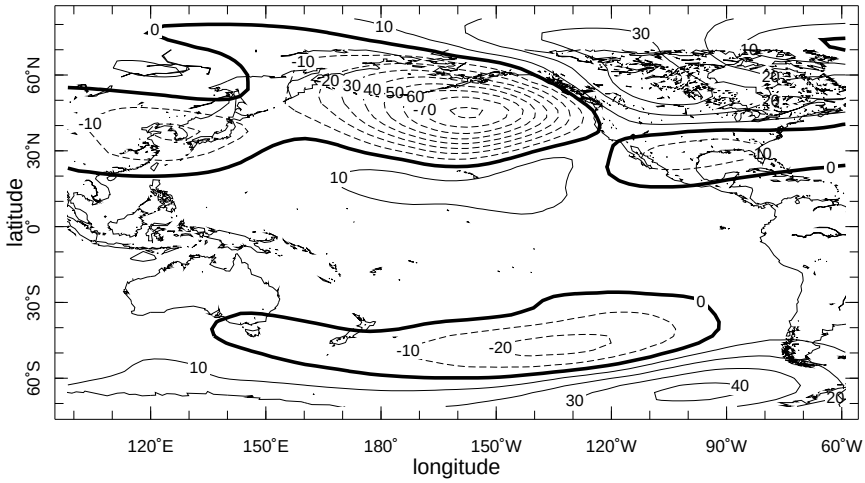

Figure 8. The decadal shift (for the same time period as in Figure 4) in 500mb height for a single CCM3 ensemble member. Units are meters. This member was chosen for its reasonable match to observations in amplitude and pattern indicating that a mix of internal and boundary-forced variability could account for the observed decadal shift.

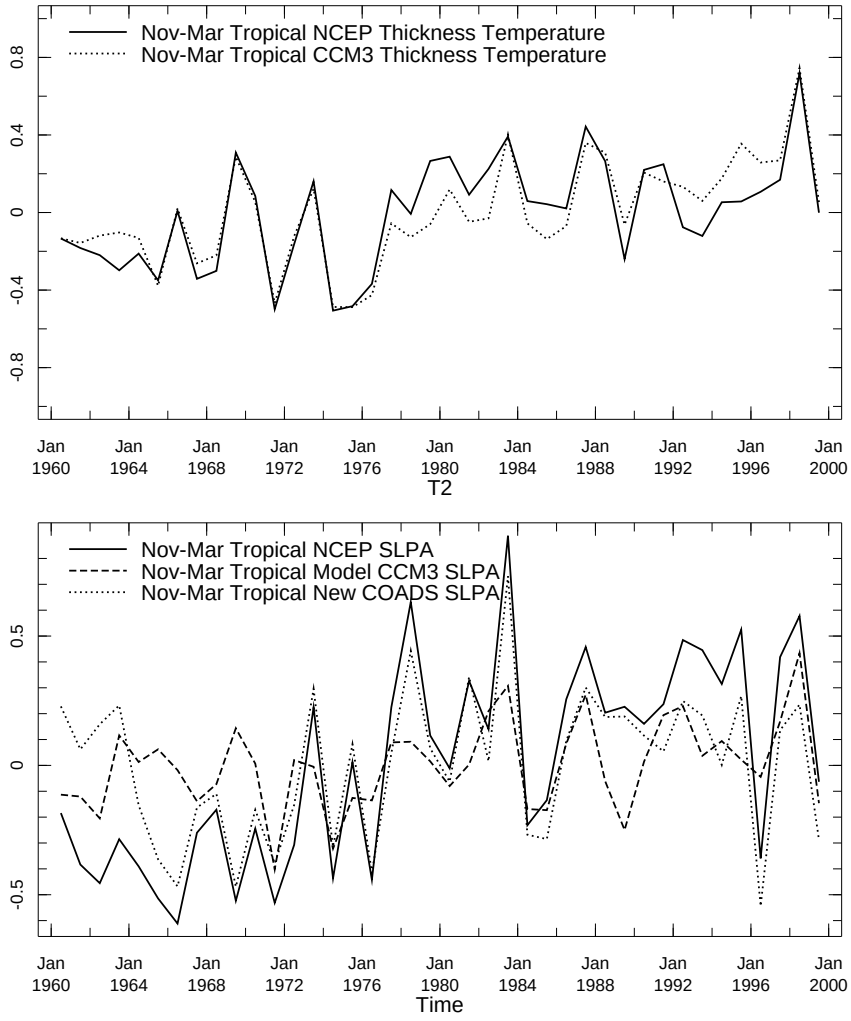

Figure 9. The tropical mean ($20°N$ to $20°S$) of (a) the thickness temperature between the surface and $500mb$ from the NCEP Reanalysis and the CCM3 model ensemble mean and (b) the SLP from NCEP Reanalysis, the CCM3 model ensemble mean and a new analysis of COADS ship data.

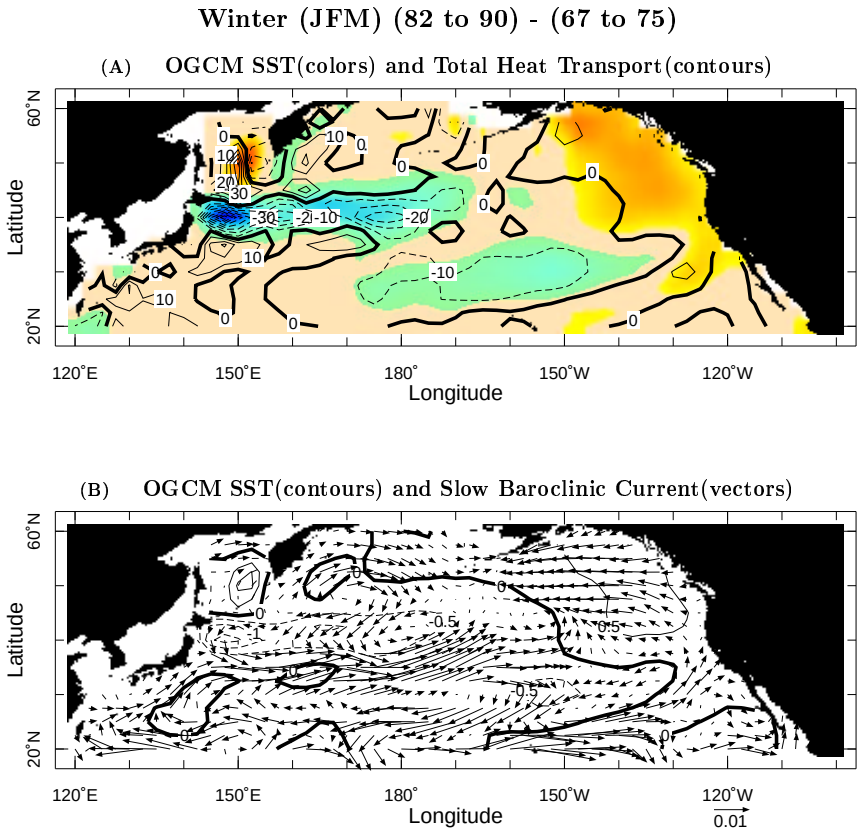

Figure 10. (a) The difference in modeled ocean heat flux convergence (contours, Wm^{-2}) and SSTs for the January to March season of the 1982 to 1990 period minus that for the 1967 to 1975 period as simulated by the ocean GCM-atmosphere mixed layer model of *Seager et al.* [2001]. The slightly later period than for the previous figures accounts for the few years timescale of gyre circulation adjustment. The strong cooling along $40°N$ is caused by a southward shift of the Kuroshio-Oyashio Extension. The shift in the slowly adjusting part (i.e. non-Ekman) part of the baroclinic circulation is shown in (b). The gyre adjustment was forced by the decadal change in the strength and location of the Aleutian Low.

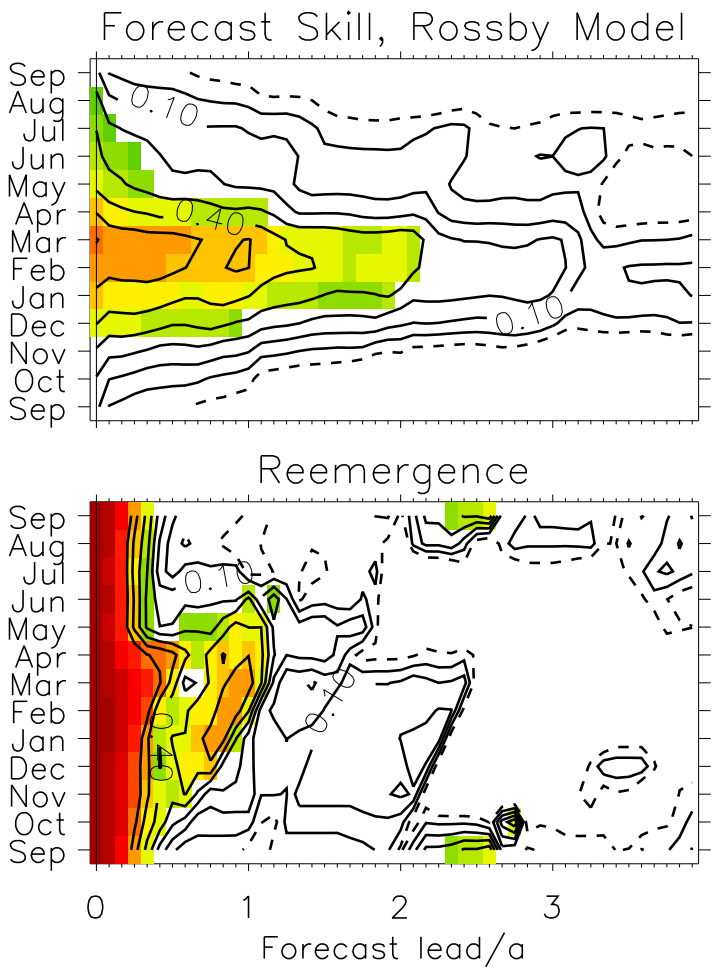

Figure 11. Skill (correlation) of hindcasts from the model of *Schneider and Miller* [2001] (top) and from the reemergence mechanism (bottom). The latter assumes that mixed layer temperature anomalies reside below the thin summer mixed layer and reemerge the following winter. Reemergence has considerable skill at lead times of one year. At longer timescales, out to almost three years, the baroclinic wave propagation model retains significant skill. Figure reproduced from *Schneider and Miller* [2001].

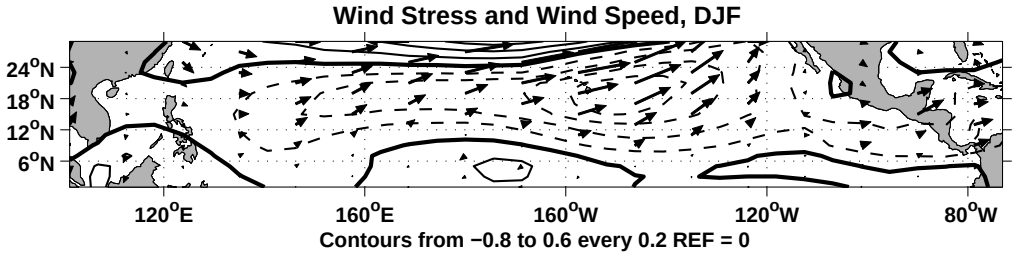

Figure 12. The pattern associated with the first singular vector of an analysis of wind stress (arrows) and wind speed (contours) within an SST-forced ensemble of atmosphere GCM integrations. Before the analysis was performed the ensemble mean, representing the SST anomaly-forced component of variability, was removed. The pattern therefore represents the dominant pattern in the model of internal atmosphere variability over the subtropical North Pacific. It accounts for 28% of the total variance in the fields.

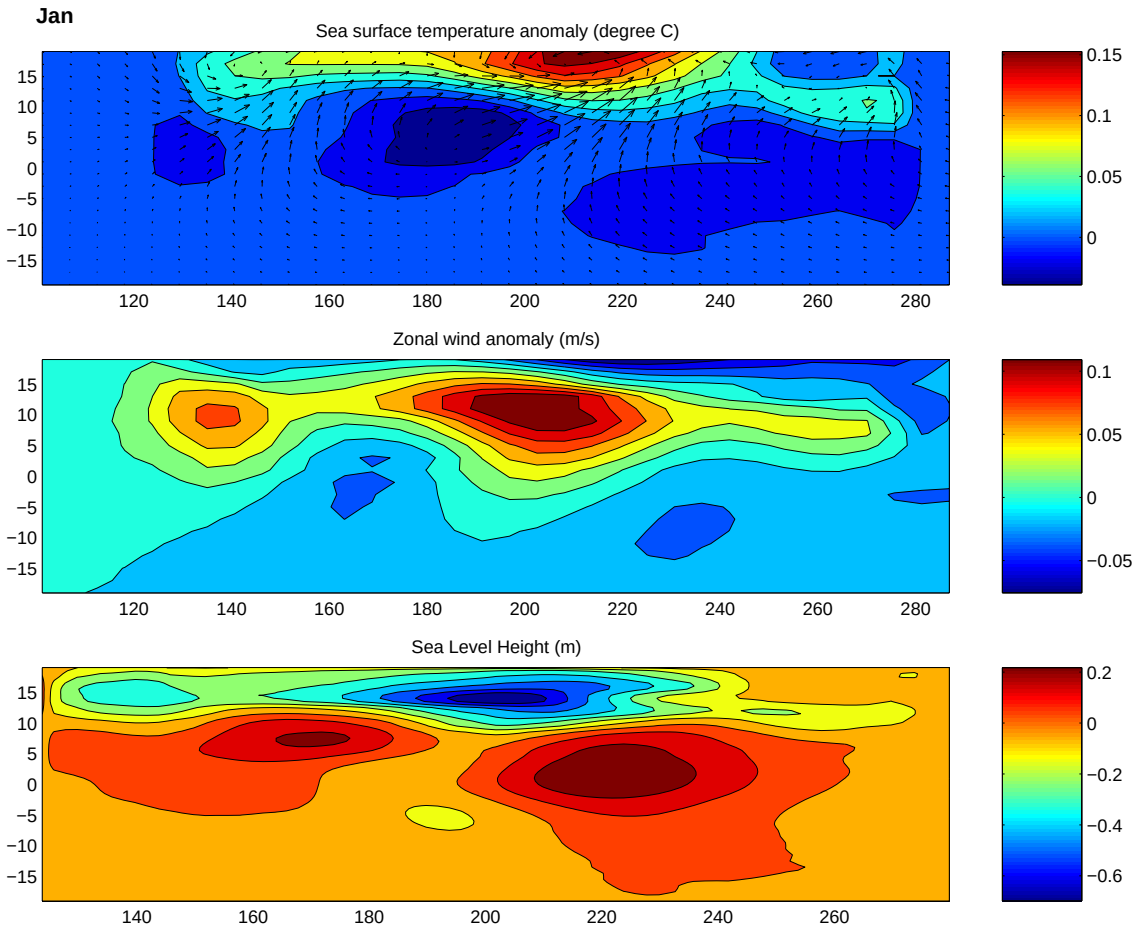

Figure 13. The response of the Zebiak-Cane model to a subtropical SST anomaly. The SST anomaly was originally generated by an imposed wind speed anomaly that begins in November and lasts through March. The figures are for the January. (a) shows the initial wind response of the model and the SST anomaly ($^{\circ}C$) which has already begun to evolve according to the model physics. (b) shows the associated zonal wind speed response (ms^{-1}) in the model and (c) the sea level height response (m).

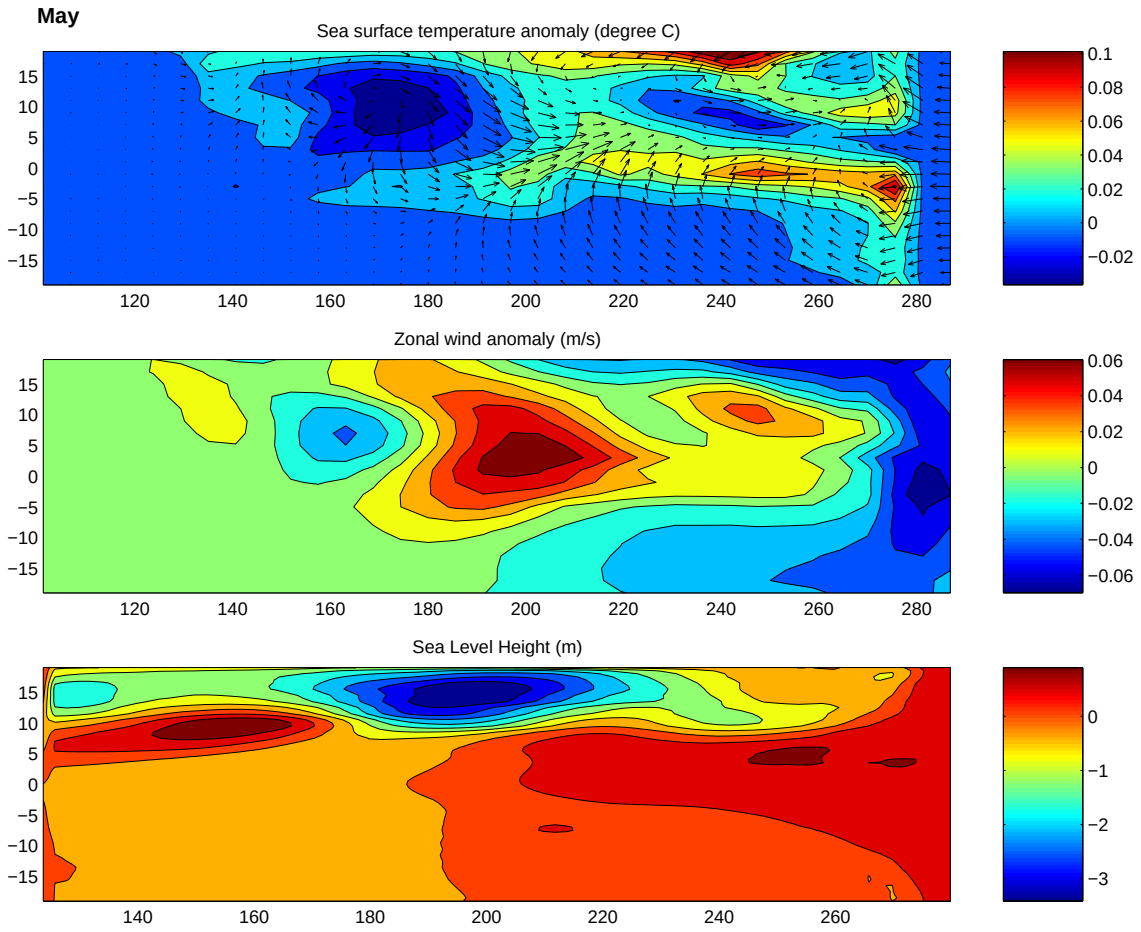

Figure 14. Same as Figure 13 but for the following May.

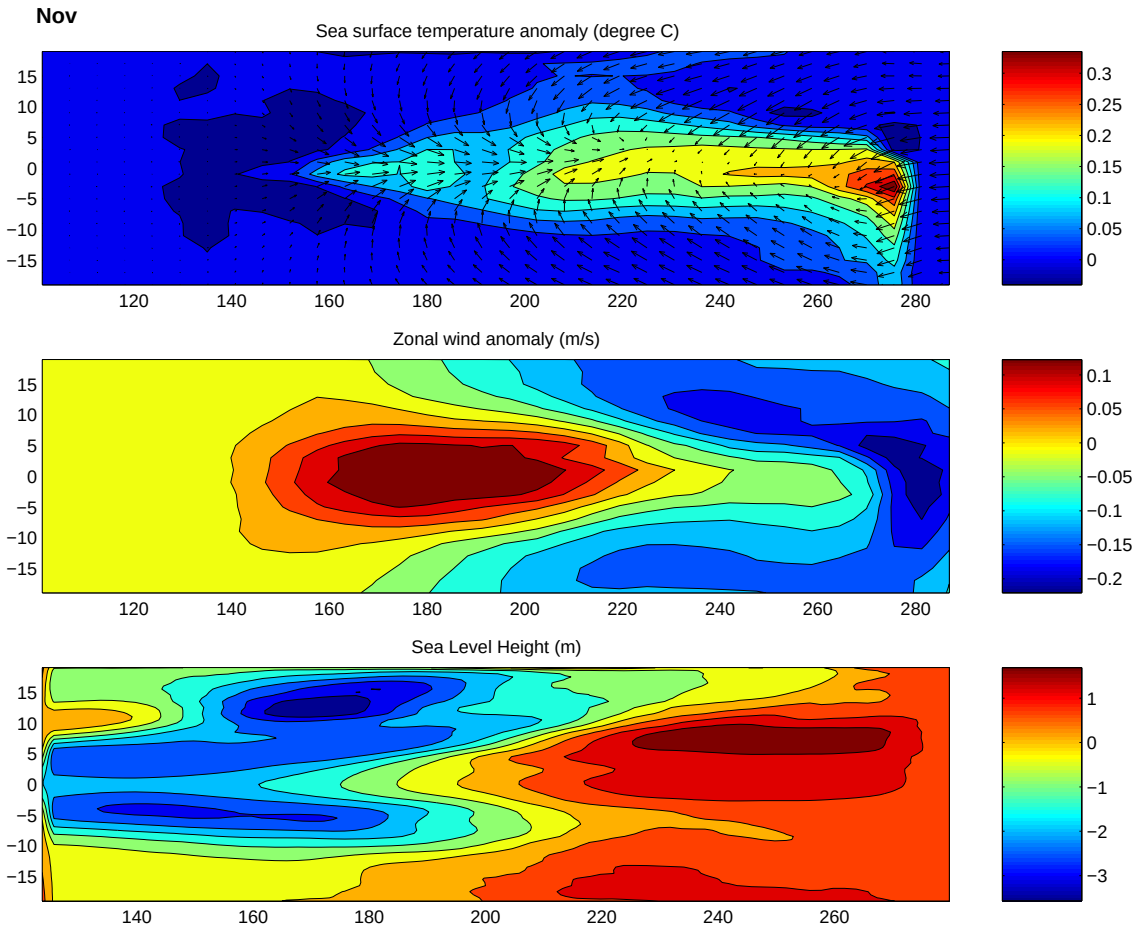

Figure 15. Same as Figure 13 but for the following November

	ZC Dynamical Forecasts			**Naive Reference Forecasts**					
				ZC-Long distribution			**AR(2)**		
	correct	*weak*	*wrong*	*correct*	*weak*	*wrong*	*correct*	*weak*	*wrong*
warm shift	54%	27%	19%	43%	24%	33%	48%	17%	35%
neutral shift	23%	42%	35%	20%	37%	43%	14%	30%	56%
cold shift	40%	24%	36%	31%	21%	48%	33%	16%	51%

Table 2. Same as Table 1, with a subtropical wind forcing imposed on the dynamical model.

References

Alexander, M. A., I. Blade, M. Newman, J. R. Lanzante, N.-C. Lau, and J. D. Scott, The atmosphere bridge: The influence of ENSO teleconnections on air-sea interaction over the global ocean, *J. Climate*, *15*, 2205–2231, 2002.

Barsugli, J. J., and P. D. Sardeshmukh, Global atmospheric sensitivity to tropcial SST anomalies throughout the Indo-Pacific basin, *J. Climate*, *15*, 3427–3442, 2002.

Basnett, T. A., and D. E. Parker, Development of the global mean sea level pressure data set GMSLP2., *Tech. Rep. 79*, Hadley Center for Climate Research, 1997.

Cane, M. A., S. E. Zebiak, and S. C. Dolan, Experimental forecasts of El Niño, *Nature*, *321*, 827–832, 1986.

Cayan, D., Latent and sensible heat flux anomalies over the northern oceans: The connection to monthly atmospheric circulation, *J. Climate*, *5*, 354–369, 1992a.

Cayan, D., Latent and sensible heat flux anomalies over the northern oceans: Driving the sea surface temperature, *J. Phys. Oceanogr.*, *22*, 859–881, 1992b.

Chen, D., M. A. Cane, S. E. Zebiak, R. Canizares, and A. Kaplan, Bias correction of an ocean-atmosphere coupled model, *Geophys. Res. Letters*, *27*, 2585–2588, 2000.

Deser, C., A. S. Phillips, and J. W. Hurrell, Pacific interdecadal climate variability: Linkages between the tropics and the North Pacific during boreal winter since 1900, *J. Climate*, 2003, submitted.

Garreaud, R. D., and D. S. Battisti, Interannual (ENSO) and interdecadal (ENSO-like) variability in the southern hemisphere tropospheric circulation., *J. Climate*, *12*, 2113–2123, 1999.

Gill, A. E., Some simple solutions for heat induced tropical circulation, *Q. J. R. Meteorol. Soc.*, *106*, 447–462, 1980.

Graham, N., Decadal-scale climate variability in the tropical and North Pacific during the 1970s and 1980s: observations and model results, *Clim. Dyn.*, *10*, 135–162, 1994.

Gu, D., and S. G. H. Philander, Interdecadal climate fluctuations that depend on exchanges between the tropics and extratropics, *Science*, *275*, 805–807, 1997.

Held, I., S. W. Lyons, and S. Nigam, Transients and the extratropical response to el niño., *J. Atmos. Sci.*, *46*, 163–176, 1989.

Hoerling, M. P., and A. Kumar, The perfect ocean for drought, *Science*, *299*, 691–694, 2003.

Hoerling, M. P., and M. Ting, Organization of extratropical transients during El Niño, *J. Climate*, *7*, 745–766, 1994.

Horel, J. D., and J. M. Wallace, Planetary scale atmospheric phenomena associated with the Southern Oscillation., *Mon. Wea. Rev.*, *109*, 813–829, 1981.

Kaplan, A., Y. Kushnir, and M. A. Cane, Reduced space optimal interpolation of historical marine sea level pressure: 1854-1992, *J. Climate*, *13*, 2987–3002, 2000.

Karspeck, A., and M. A. Cane, Tropical Pacific 1976/77 climate shift in a linear wind-driven model, *J. Phys. Oceanogr.*, *32*, 2350–2360, 2002.

Karspeck, A., R. Seager, and M. A. Cane, Predicting decadal variability of the tropical Pacific with an intermediate model, *J. Climate*, 2003, to be submitted.

Kiehl, J. T., J. J. Hack, G. B. Bonan, B. A. Bovile, D. L. Williamson, and P. J. Rasch, The National Center for Atmospheric Research Community Climate Model: CCM3, *J. Climate*, *11*, 1131–1149,

1998.

Klein, S. A., B. J. Soden, and N. Lau, Remote sea surface temperature variations during ENSO: Evidence for a tropical atmospheric bridge, *J. Climate*, *12*, 917–932, 1999.

KrishnaKumar, K., B. Rajagopolan, and M. A. Cane, On the weakening relationship between the Indian monsoon and ENSO, *Science*, *284*, 2156–2159, 1999.

Krishnamurthy, V., and B. N. Goswami, Indian monsoon-ENSO relationship on interdecadal timescale, *J. Climate*, *13*, 579–595, 2000.

Latif, M., and T. P. Barnett, Causes of decadal climate variability over the North Pacific/North American sector, *Science*, *266*, 634–637, 1994.

Latif, M., and T. P. Barnett, Decadal climate variability over the North Pacific and North America: Dynamics and predictability, *J. Climate*, *9*, 2407–2423, 1996.

Mantua, N. J., S. R. Hare, Y. Zhang, J. M. Wallace, and R. C. Francis, A Pacific interdecadal climate oscillation with impacts on salmon production, *Bull. Amer. Meteor. Soc.*, *78*, 1069–1079, 1997.

McPhaden, M. J., and D. Zhang, Slowdown of the meridional overturning circulation in the upper Pacific Ocean, *Nature*, *415*, 603–608, 2002.

Miller, A. J., and N. Schneider, Interdecadal climate regime dynamics in the North Pacific Ocean: Theories, observations and ecosystem impacts, *Prog. Oceanogr.*, 2001, submitted.

Miller, A. J., D. R. Cayan, T. P. Barnett, N. E. Graham, and J. M. Oberhuber, Interdecadal variability of the Pacific Ocean: Model response to observed heat flux and wind stress anomalies, *Clim. Dyn.*, *9*, 287–302, 1994.

Nakamura, H., G. Lin, and T. Yamagata, Decadal climate variability in the North Pacific during the recent decades, *Bull. Amer. Meteor. Soc.*, *78*, 2215–2225, 1997.

Pierce, D. W., T. P. Barnett, and M. Latif, Connections between the Pacific Ocean tropics and midlatitudes on decadal timescales, *J. Climate*, *13*, 1173–1194, 2000.

Power, S., F. Tseitkin, V. Mehta, B. Lavery, S. Trock, and N. Holbrook, Decadal climate variability in Australia during the twentieth century, *Int. J. Climatology*, *19*, 169–184, 1999.

Rayner, N., D. Parker, E. Horton, C. Folland, L. Alexander, D. Rowell, E. Kent, and A. Kaplan, Global analyses of sea surface temperature, sea ice, and night marine air temperature since the late nineteenth century, *J. Geophys. Res.*, *108*, 10.1029/2002JD002,670, 2003.

Ropelewski, C. F., and M. S. Halpert, Global and regional scale precipitation patterns associated with the El Niño/Southern Oscillation., *Mon. Wea. Rev.*, *114*, 2352–2362, 1987.

Ropelewski, C. F., and M. S. Halpert, Precipitation patterns associated with the high index phase of the southern oscillation, *J. Climate*, *2*, 268–284, 1989.

Sardeshmukh, P. D., and B. J. Hoskins, The generation of global rotational flow by steady idealized tropical divergence, *J. Atmos. Sci.*, *45*, 1228–1251, 1988.

Schneider, N., and A. J. Miller, Predicting western North Pacific Ocean climate, *J. Climate*, *14*, 3997–4002, 2001.

Schneider, N., S. Venzke, A. J. Miller, D. W. Pierce, T. O. Barnett, C. Deser, and M. Latif, Pacific thermocline bridge revisted, *Geophys. Res. Letters*, *26*, 1329–1332, 1999.

Seager, R., S. E. Zebiak, and M. A. Cane, A model of the tropical Pacific sea surface temperature climatology, *J. Geophys. Res.*, *93*, 1265–1280, 1988.

Seager, R., Y. Kushnir, N. Naik, M. A. Cane, and J. Miller, Wind-driven shifts in the latitude of the Kuroshio-Oyashio extension and generation of SST anomalies on decadal timescales, *J. Climate*, *14*, 4249–4265, 2001.

Seager, R., N. Harnik, Y. Kushnir, W. Robinson, and J. Miller, Mechanisms of hemispherically symmetric climate variability, *J. Climate*, *16*, 2960–2978, 2003.

Trenberth, K., and J. W. Hurrell, Decadal atmosphere-ocean variations in the Pacific, *Clim. Dyn.*, *9*, 303–319, 1994.

Tziperman, E., M. A. Cane, and S. E. Zebiak, Irregularity and locking to the seasonal cycle in an enso prediction model as explained by the quasi-periodicity route to chaos, *J. Atmos. Sci.*, *52*, 293–306, 1995.

Vimont, D., D. S. Battisti, and A. C. Hirst, Footprinting: a seasonal link between the mid-latitudes and tropics, *Geophys. Res. Letters*, *28*, 3923–3926, 2001.

Vimont, D., J. M. Wallace, and D. S. Battisti, The seasonal footprinting mechanism in the Pacific; implications for ENSO, *J. Climate*, *16*, 2668–2675, 2003.

Wilks, D. S., *Statistical methods in the atmospheric sciences.*, Academic Press, San Diego, 467pp, 1995.

Woodruff, S., R. Slutz, R. Jenne, and P. Steurer, COADS Release 2: Data and Metadata Enhancements for Improvements of Marine Surface Flux Fields, *Phys. Chem Earth*, *23*, 517–527, 1998.

Zebiak, S. E., A simple atmospheric model of relevance to El Niño., *J. Atmos. Sci.*, *39*, 2017–2027, 1982.

Zebiak, S. E., and M. A. Cane, A model El Niño-Southern Oscillation, *Mon. Wea. Rev.*, *115*, 2262–2278, 1987.

Zhang, Y., J. M. Wallace, and D. S. Battisti, ENSO-like decade-to-century scale variability: 1900-93, *J. Climate*, *10*, 1004–1020, 1997.